

A Cost Effective Solar Charge Controller and Load Driver for DC Home Appliances

A.A. Willoughby¹, O.A. Babalola²

¹ Department of Physics, Covenant University, Ota, Ogun State, Nigeria

² Department of Physics, University of Ilorin, Ilorin, Kwara State, Nigeria

Abstract: The cost effective circuit presented is a simple solution to frequent blackouts experienced in homes throughout Nigeria. It is basically a solar charge controller comprising two different switching circuits for battery charging and DC load driving, using readily available and cheap components. A TL494 switch mode IC is configured as a DC-DC buck converter and its duty cycle used to control the switching of a Sziklai pair of output transistors for charging a sealed lead acid battery. The two error amplifiers in the chip are used to set the output voltage and to implement current limiting respectively. The voltages at the non-inverting inputs of both error amplifiers during the charging process are monitored and logged at three minute intervals with a data logger to observe the charging process. A 555 timer oscillator and a power MOSFET driven by a push-pull low power complementary transistor pair are used for power switching of DC loads such as fans or LED bulbs.

Keywords: Charge Controller, Constant Current-Constant Voltage, DC-DC Buck Converter, Duty Cycle, Solar LED Lighting.

I. Introduction

Nigeria's intractable electricity power crisis has been ongoing for decades. This is a consequence of inherent problems in the sectors of generation, transmission and distribution. Systematic failure has resulted in incessant power cuts, blackouts and unhealthy mains which have adversely affected offices, businesses and homes. The country now generates less than 25 % installed capacity [16]. Most homes can be without electricity for days and the alternatives to lighting are the traditional candle light, kerosene lamps, petrol/diesel generators or an inverter, if it is affordable. The first three are carbon emitters, run the risk of fire hazard, and in the case of the generator, noise polluter as well, all contributing to respiratory problems and environmental degradation.

In order to reduce carbon footprints as well as mitigate climate change, the whole world is gradually switching to renewable energy for alternative energy supply in an effort to diminish total reliance on fossil fuels. It is essential that Nigeria be at the vanguard of renewable energy consumers and harness the sun's abundant energy for its energy demands because of the following reasons: its non functioning refineries and perennial gas crisis, total reliance on fuel imports and unpredictable fuel price fluctuations affecting its economy, the exorbitant cost of fueling and maintaining petrol/diesel generators on a daily basis and lastly, its natural endowment of renewable energy resources by virtue of its location very near the equator. Nigeria is a tropical country situated between 3°E to 14°E of longitude and 4°N to 14°N of latitude and supplied with ample amount of sunlight all year round; it has an annual average daily solar radiation of about 5.25 kWh/m² per day varying between 3.5 kWh/m² per day at the coastal areas and 7.0 kWh/m² per day at the Northern boundary, and an annual average daily sunshine of 6.25 hrs ranging between 3.5 hrs at the coastal areas and 9.0 hrs at the far northern boundary [15].

This work is one of several contributions intended to tackle the problem of blackouts, especially in rural settings, where the grid is nonexistent. With the development and availability of low-priced, very efficient DC LED bulbs, a household can be conveniently lit with these bulbs from a battery charged by a solar panel during the day. A 3 watt DC LED bulb is equivalent in output to a 45 watt incandescent bulb, has much higher lumens per watt compared to the 11 watt energy saving fluorescent bulbs and generates much less heat. They light up immediately, attaining full intensity instantaneously and their performance and life span are not affected by frequent on and off cyclic switching. Consequently, they can be dimmed using pulse width modulation [17]. Substantial energy savings is guaranteed from utilization of these bulbs. A home might wish to do away with AC lighting completely, independent of the grid, by wiring lines separately for DC appliances such as LED bulbs, fans, mobile phone charging, etc. To achieve this, an affordable but efficient solar charger is needed to charge deep cycle batteries during the sun hours of the day and the stored energy discharged into lighting rooms in the home. Charge controllers are designed to prevent battery from being overcharged and also to disconnect loads when being over discharged [14]. Branded Pulse Width Modulation (PWM) and Maximum Power Point Tracking (MPPT) designs are the more efficient types for converting solar power for battery charging, but they are expensive. PWM circuits operate at fixed frequency and regulate the output voltage by adjusting the output switching transistor's duty cycle.

The work discussed in this paper comprises two different switching circuits. The first, a battery charger, is based on the ‘ancient’ cheap TL494 switch mode chip configured as a constant current, constant voltage (cc-cv), DC-DC buck converter. The second is a switch mode driver for powering DC loads using an equally inexpensive and common chip, the 555 timer. From a budgetary viewpoint, the components are cheap, versatile and their manufacture not discontinued. The product as a whole is inexpensive, and can be used at the household level, with particular attention to rural dwellers, low income earners as well as those on higher salary scales.

II. Circuit Details

Fig.1 shows the block diagram of the controller comprising of the PV module, cc-cv charger, the deep cycle battery and the PWM load driver. Fig.2 shows the circuit diagram of the charger.



Fig. 1 Block Diagram of the Charge Controller

2.1. The charger

Literature on the internal configuration and pin functions of the chip are outlined in the following articles: [1], [2], [3] and [4]. The TL494 (IC1) is a fixed frequency pulse-width-modulation (PWM) controller containing two error amplifiers, a sawtooth waveform generator and a 5 V reference, V_{REF} . It also contains a dead time control comparator, and output control options for single ended or push-pull action. Single ended operation has been utilized in this circuit. The circuit is configured as a step-down (buck) switching converter, where a voltage source, say a 22 V solar module is converted to a lower regulated voltage of about 14 V. A 12 V battery directly connected to a 22 V solar module will pull the module’s operating voltage down to battery voltage level but if a DC-DC step down buck converter is coupled in between them, higher pulsed power can be transferred from the module to the battery with minimal power loss. Since the input voltage from the panel will rise past 20 V, ZD1 serves as gate protection for the power MOSFET, IRF9540. The compound duo of Q2 and Q3 or Sziklai pair configuration behaves like a transistor with large beta gain and provides output charging current. Total gain $\beta = \beta_{Q2} * \beta_{Q3}$. The main parameters required in the design of a step-down converter are: the switching frequency, input voltage range, fixed output voltage and output current.

2.2 Buck converter operation

Discussion on the theory and functionality of buck converter topology and design equations for calculating required parameters can be found in the following references, [5],..... [10]. Referring to Fig.2, a summary explanation is as follows: current from the solar module flows through diode D2 into transistor Q3. When Q3 is turned on by a rising pulse, i.e. at t_{ON} , current from the module is allowed to flow through the inductor L1 into the output capacitor C4 as well as the battery. As this current rises at the rate of $\Delta I/\Delta t = V/L$, the magnetic field of the inductor also increases. This magnetic energy is stored in the coil. At t_{OFF} , Q3 is turned off. Consequently, the peak current decays at a rate of $\Delta I/\Delta t = V/L$ as energy is transferred to C4 and the battery.

The magnetic field in the inductor also begins to collapse; a reverse voltage is then generated that forward biases the fast recovery Schottky diode, D4. The energy stored in the coil is then released into C4 and the battery.

2.3 Design Parameters

Taking required operating parameters as:

Solar module output voltage, $V_{IN} = 22$ V, Converter output, $V_{OUT} = 14.4$ V,

$$P_{OUT} = V_{OUT} \times I_{OUT} = 14.4 \text{ V} \times 10 \text{ A} = 144 \text{ W} \tag{1}$$

$$I_{OUT(\min)} = 10 \% \text{ of } I_{OUT} = 1 \text{ A} \tag{2}$$

$$V_{pp_ripple(\max)} = 1 \% \text{ of } V_{OUT} = 0.144 \text{ V} \tag{3}$$

2.3.1 Oscillator Frequency, f_{osc}

Resistor R8 (39 k Ω) and capacitor C1 (1nF) at pins 5 and 6 respectively, set the internal oscillator frequency, i.e.

$$f_{osc} = \frac{1}{R8 \times C1} = \frac{1}{39 \times 10^3 \times 1 \times 10^{-9}} \approx 25 \text{ kHz} \quad (4)$$

$$\text{Switching Period, } T = \frac{1}{f_{osc}} \approx 40 \mu\text{s} \quad (5)$$

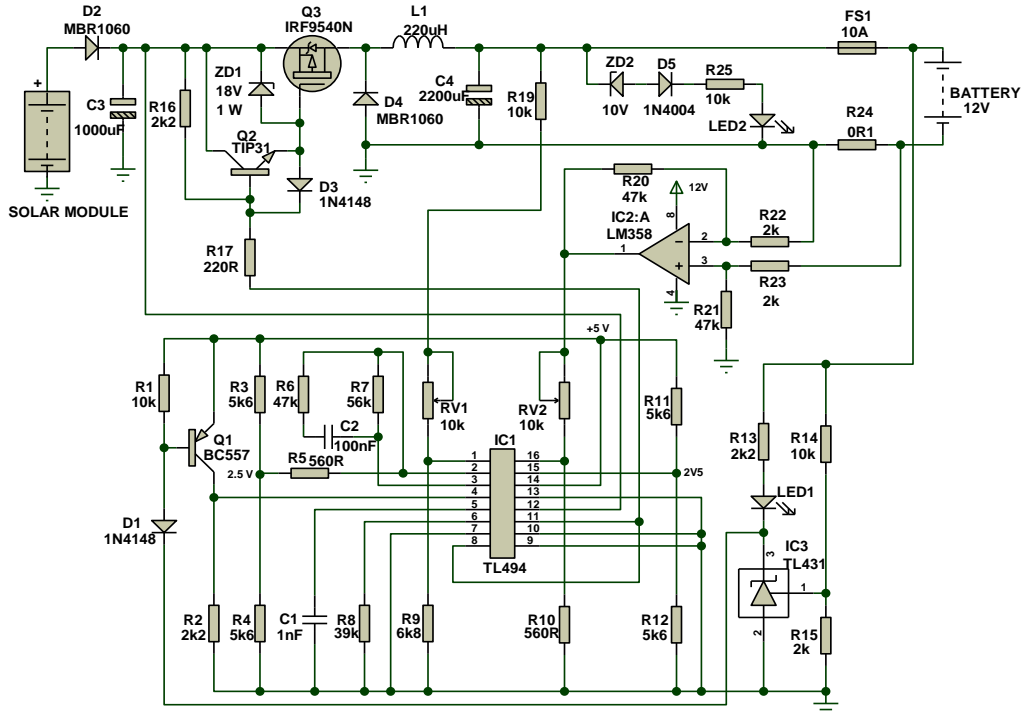


Fig.2 Circuit diagram of the dc-dc buck converter

The transfer function of the buck converter is as a function of the duty cycle, D, as:

$$D = \frac{V_{OUT}}{V_{IN}} = \frac{V_{OUT} + V_F}{V_{IN} - V_{RDS(on)}} = \frac{14.4 + 0.8}{22 - 1.17} = 0.73 \quad (6)$$

where V_F is the forward voltage drop (0.8 V) across the Schottky diode, MBR1060, $R_{DS(on)}$ is the on resistance (0.117 Ω) of the MOSFET, IRF9540N, $V_{RDS(on)}$, the voltage drop across $R_{DS(on)} = 0.117 \Omega \times 10 \text{ A} = 1.17 \text{ V}$. But Duty cycle,

$$D = \frac{t_{ON}}{t_{ON} + t_{OFF}} = \frac{t_{ON}}{T} = \frac{t_{ON}}{40 \mu\text{s}} \quad (7)$$

$$t_{ON} = \frac{D}{f_{osc}} = D \cdot T = 0.73 \times 40 \mu\text{s} \approx 29 \mu\text{s} \quad (8)$$

$$t_{OFF} = \frac{1}{f_{osc}} - t_{ON} = T - t_{ON} \approx 11 \mu\text{s} \quad (9)$$

t_{ON} and t_{OFF} are the times for which the output driver transistor switches on and off respectively.

2.3.2 Inductor Selection

$$L = \frac{V_{OUT} \times (V_{IN} - V_{OUT})}{\Delta I_L \times f_{osc} \times V_{IN}} = \frac{14.4 \times (22 - 14.4)}{0.2 \times 10 \times 25 \times 10^3 \times 22} \approx 100 \mu\text{H} \quad (10)$$

Where ΔI_L is the inductor ripple current, which is 20% to 40 % of the output current [1], [2], i.e. $\Delta I_L = (0.2 \text{ to } 0.4) \times I_{OUT(max)}$.

2.3.3 Peak Switch Current

$$I_{PEAK} = I_{OUT} + I_{MIN} = 10 + 1 = 11A \tag{11}$$

2.3.4 Diode Selection

The forward current rating should be equal to the maximum output current, i.e.,

$$I_F = I_{OUT(max)} \times (1 - D) = 10 \times (1 - 0.729) = 2.7 A \tag{12}$$

The power dissipation of the diode is then $P_D = I_F \times V_F = 2.7 \times 0.8 = 2.2 W$. The characteristics of the MBR1060 Schottky are adequate in meeting the calculated values above.

2.3.5 Output Capacitor Selection

Output capacitor C4 is selected using a low ESR (Equivalent Series Resistance), [1], [5]:

$$C_{OUT} = \frac{\Delta I_L}{8 \times f_{osc} \times V_{pp_ripple(max)}} \approx \frac{0.2 \times 10}{8 \times 25 \times 10^3 \times 0.144} \approx 70 \mu F \tag{13}$$

2.4 Constant voltage (cv) – set by Error-amp1

Error amp1, shown in Fig.3 is used to control and fix the output voltage at a constant value of 14.4 V. It samples the output voltage, compares it to the 2.5 V reference voltage and adjusts the PWM to maintain a constant output voltage. The amplifier has its non-inverting and inverting inputs at pins 1 and 2, respectively. A potential divider network consisting of R19, RV1 and R9 attenuates the output voltage to about 2.5 V, feeding it to the non-inverting input pin 1. The inverting input, pin 2, is fixed at half (2.5 V) the value of the IC’s internal 5 V reference at pin 14. When the output voltage rises, so that pin 1 voltage rises above the reference 2.5 V at pin 2, the output of the error-amplifier also rises and this in turn reduces the pulse width outputs at pins 8 & 11.

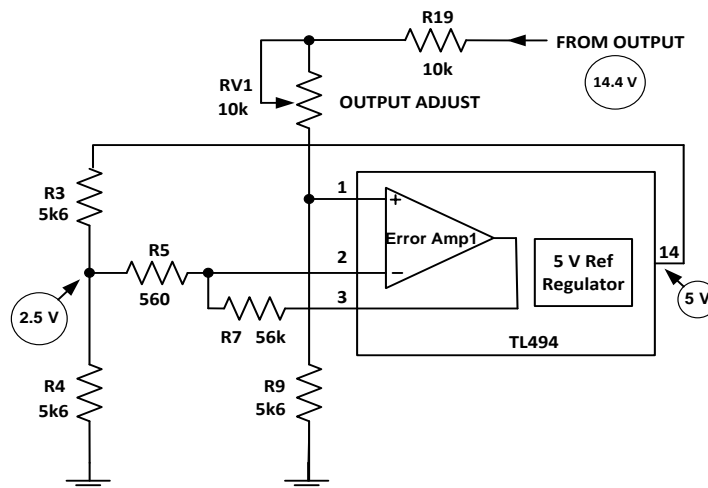


Fig.3 Output voltage monitoring

Conversely, if the output falls, such that pin 1 voltage drops below 2.5 V, the error amp output reduces and the pulse width is then forced to increase. The output voltage is regulated to about 14.4 V with RV1. The stability of the error- amplifier circuit is improved by R7 feedback resistor between pins 3 and 2. With the resistor values shown, the gain is set to about 100.

2.5 Constant current (cc) provided by Error Amp2

In Fig. 4, one half of an LM358 op amp is used in a low-side current sensing mode. A differential voltage generated across the external sense resistor shunt, R24 (0.1Ω), inserted in series with the current path is amplified by the op amp; the amplified output signal is used to control the charging current. As the battery is being charged, the differential voltage appearing between pins 2 and 3 of LM358 is amplified by the op amp which has a gain of $A_v = R20/R22 = 24$. A reference voltage of about 2.5 V is set by R11 and R12 at the inverting input pin 15 of the TL494. Pin 16 can be adjusted to approximately 2.5 V using RV2 and a fully

charged battery at 14.4 V. As a flat battery being charged approaches full charge, voltage at pin 16 approaches 2.5 V so that pulses at pins 8 & 11 and consequently charging current reduced.

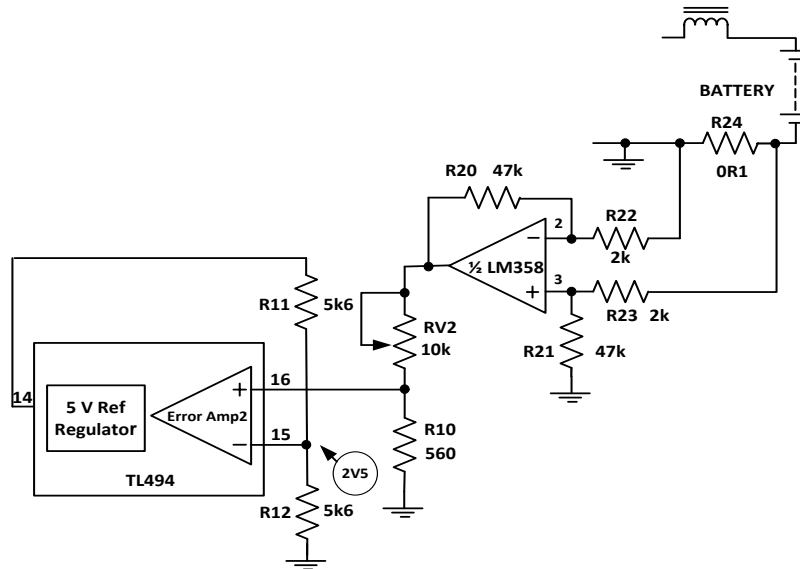


Fig.4 Battery current sensing

2.6 Overvoltage protection

The dead-time comparator, with its input at pin 4, is usually used to ensure that there is a short delay between one output (pin 8) going high and the other (pin 11) going low. In this design, it is used to monitor overvoltage condition [2]. A TL431 shunt regulator is the sensing element. If the output voltage should increase to the point that 2.5 V is developed at the reference node, V_{REF} , of the TL431, the device conducts, causing its cathode to drop close to 0 V. Q1 becomes forward biased and pulls pin 4 high, up to V_{REF} , disabling the output transistors and hence shutting down IC1's output pulses. Resistors R14 and R15 monitor this output voltage, fixing V_{REF} at 2.5 V. Under normal safe voltage, pin 4 is low, approximately 0 V, so that the dead-time decreases to a minimum and the output pulses are increased. The value of R15 is calculated thus, [11]:

$$V_{OUT} = \left(1 + \frac{R14}{R15}\right) V_{REF}, \text{ i. e., } 14.4 = \left(1 + \frac{10k}{R15}\right) 2.5; \quad R15 \approx 2.1k\Omega \quad (14)$$

LED2 is a charge indicator. Current through it is provided by R25 via ZD2, and D5.

2.7 Output drive transistors

A compound transistor pair, Sziklai configuration is driven by the TL494 switch mode chip which has a feedback network comprising R19, RV1 and R9 to keep the stepped down voltage from the module fixed at about 14.4 V. This feedback controls the duty cycle and hence the width of the pulses applied to the base of the driver transistor Q2 (TIP31) in the Sziklai pair.

3 DC Load Driver circuit

Fig.5 shows the circuit that can be used to drive a DC load (i.e., DC LED bulbs).

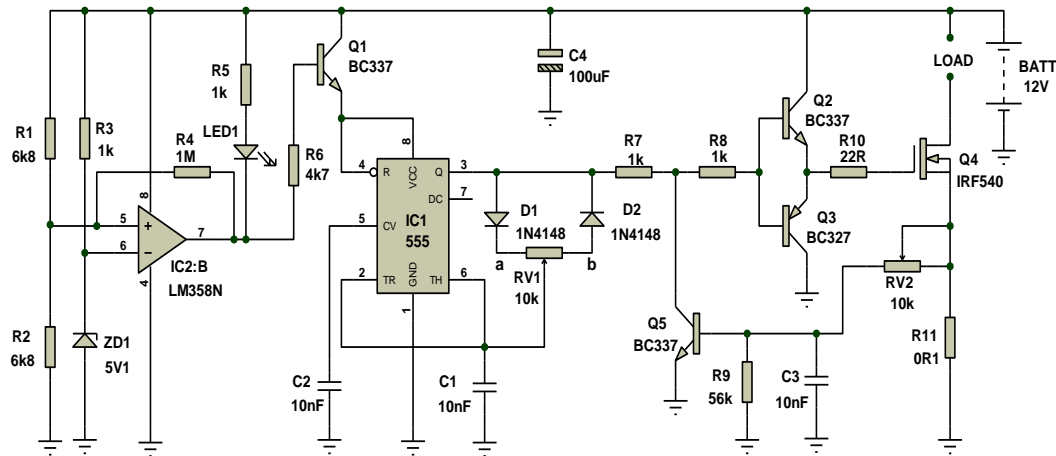


Fig.5 DC Load driver circuit

The above design easily facilitates the control of the current flowing through the LEDs and hence controls the brightness and dimming [13]. Pulse Width Modulation, PWM, method provides an efficient method of achieving this. The LEDs are turned on and off at a very high frequency such that the strobing effect is not easily perceived. IC1 is a 555 timer chip arranged as an oscillator. Capacitor C1 (10nF) connected to pins 2 and 6 is charged and discharged via the output pin 3 through diodes D1 and D2 and potentiometer RV1. RV1 serves to control power delivered by the MOSFET to the load. Output pin 3 is a high current drive for loads. Assuming it is in the high state, its voltage is approximately 1.7 less than the supply voltage. This voltage charges capacitor C1 via diode D1 in series with the 'a' side of RV1 connected between cathode of D1 and the wiper of RV1. Pins 2 and 6 are the inverting and non-inverting inputs to the lower and upper comparators in the 555 respectively. While pin 2 is used to set the latch which causes the output to go low, then pin 6, the threshold terminal, resets the latch and causes the output pin 3 to toggle low when it sees a voltage of $\frac{2}{3}$ of supply voltage, [12]. When pin 3 goes close to 0 V, it discharges capacitor C1 via diode D2 and the 'b' side of RV1 between its wiper the anode of D2. The moment the voltage of the discharged C1 reaches $\frac{1}{3}$ of the supply, it is detected by pin 2 which sets the latch and causes pin 3 to toggle high so that the charging process starts all over again. The rate of charge and discharge of C1 is dependent on values of C1 and RV1. Setting RV1 wiper to the middle position divides total resistance of RV1 equally and thus sets the duty cycle, D, to 50 %, so that C1 is charged and discharged at equal times, i.e.

$$D = \frac{t_{ON}}{T} = 50\% \quad (15)$$

where the period, $T = t_{ON} + t_{OFF}$

Therefore, to obtain times for which the output is high or low for certain lengths of time, i.e. different duty cycles, RV1 is varied but the frequency does not change since $f = \frac{1}{T}$ and $T = t_{ON} + t_{OFF}$.

$$f = \frac{1}{T} = \frac{1}{0.693 \times C1 \times RV1} = \frac{1}{0.693 \times 10 \times 10^{-9} \times 10 \times 10^3} = 14430 \text{ Hz} \quad (16)$$

If LED bulbs are to be driven loads, RV1 is then used to control the brightness or dimness by increasing or decreasing the duty cycle respectively. For a 90 % duty cycle, MOSFET conduction is continuous and the LEDs remain bright, while a 10 % duty cycle reduces the brightness. Q5, RV2 and R11 monitor the load currents. Push-pull totem pole buffer arrangement of transistors Q2 and Q3 drives the gate of the MOSFET Q4, which in turn drives the DC loads. Q5 serves as current limiting and monitors the drive currents into the load. As load currents increase, 0.7 V developed across R11 switches on Q5 which in turn reduces drive currents into the push- pull pair of Q2/Q3 and hence into Q4.

The other half of LM358 op amp (IC2:B), is a low battery voltage detector to prevent total battery discharge. When battery voltage falls below 11 V, then pin 6 would have dropped below 5V1 reference voltage as fixed by Zener diode ZD1 at pin 5. Output pin 7 will toggle low, switching off Q5 thus disabling the 555 timer and switching off drive to the load. R4 provides some hysteresis so prevent false triggering. LED1 is the low battery indicator which switches on when output pin 7 goes low.

III. Results

Fig. 6 shows the I-V and P-V curves of a 60 W panel ($I_{sc} = 3.2 \text{ A}$, $V_{oc} = 22 \text{ V}$) used to power the circuit. The characteristics curves were obtained using an I-V curve tracer designed by Ref. [18]. The experiments were carried out on the rooftop of the Department of Physics, Covenant University, Ota, Nigeria. On a typical day, 24/06/2015, and at a low insolation level of 450 W/m^2 , short circuit current of 1.4 A and maximum power point of 20 W is obtainable, i.e., enough input current into the controller for sufficient charging. A Pace XR5 datalogger was used to log the PV and battery voltages as well as voltages appearing at the TL494 pins 1 and 16, at 3-minute intervals. Fig.7 shows the daytime variations of the PV and battery voltages. In Fig.8, charging is observed from morning (09:15) till sunset by comparing the voltages appearing at the non-inverting inputs of the error amplifiers of the TL494's pins 1 and 16. As the battery voltage rises, charging current from the charger decreases. When the current demand reduces to mA range, output voltage switches to float voltage, preventing overcharge. Over voltage circuit comprising TL431 and BC557 clips the voltage at approximately 14.4 V further preventing the circuit from overcharging.

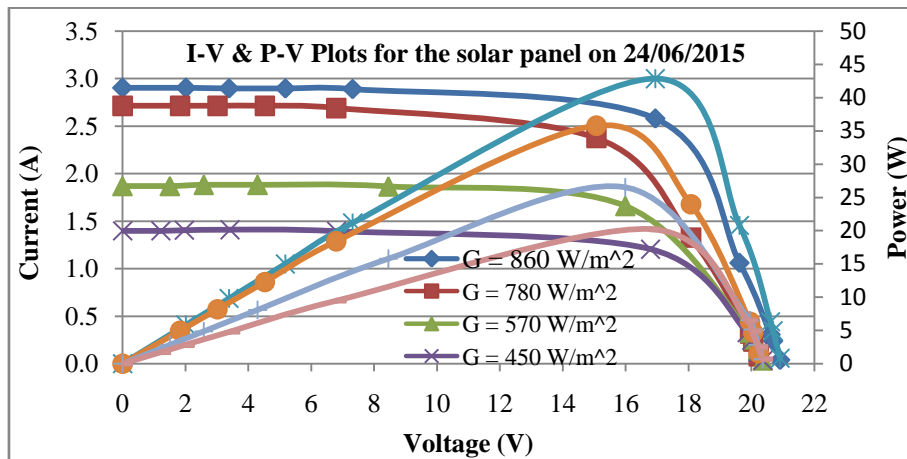


Fig.6 Current-Voltage and Power-Voltage characteristics of the 60 W solar panel

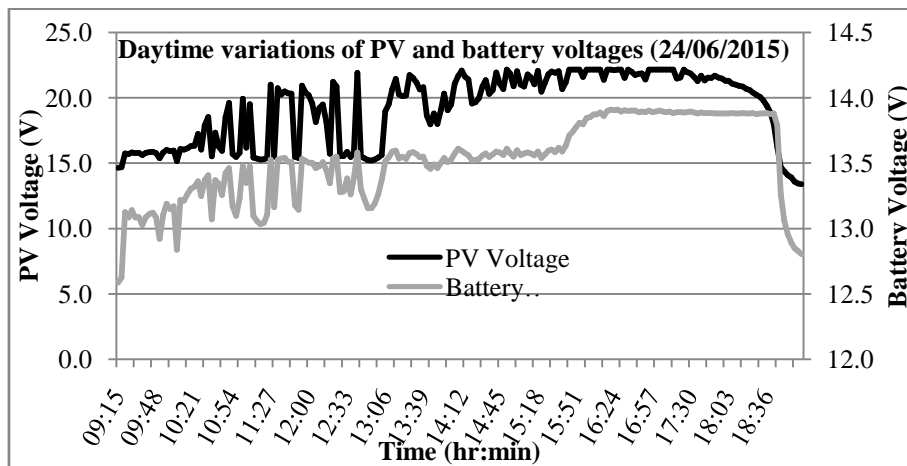


Fig.7 Three minute variations of simultaneous monitoring of PV and battery voltages

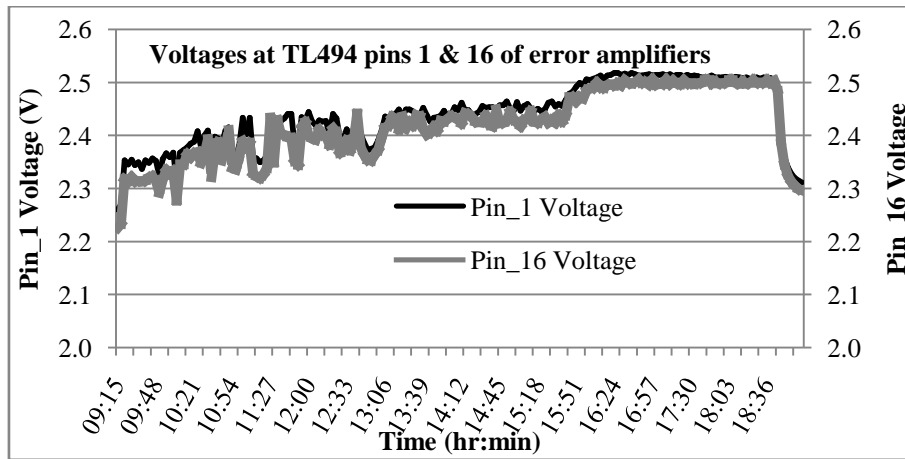


Fig. 8 Observed voltages at non inverting input pins 1 & 16 of the error amplifiers during charging.

Fig 9 illustrates the rate of decrease of the battery voltage while powering ten LED bulbs simultaneously in six hours from 18:30 to 00:30. The battery used was a 12 V Powersafe Exide type with a C rating of 17 Ah. Theoretically, 1 A is discharged in 17 hours. Supposedly, ten LED bulbs consuming 2.5 A from a 17 Ah battery will result in a discharge time in about 6.2 hrs ($t = C/I^n$), assuming Peukert exponent $n = 1.1$. The exponent n , demonstrates how well the battery performs under high discharge rates. After six hours of lighting, battery voltage reads a little above 11.5 V. The low battery voltage detector is set to 11 V, to prevent the depth of discharge, DOD, to be maintained to not more than 50 %, by disabling the driver from the load. This allows for longer cycles – periods of discharge and recharge, so the battery life is increased.

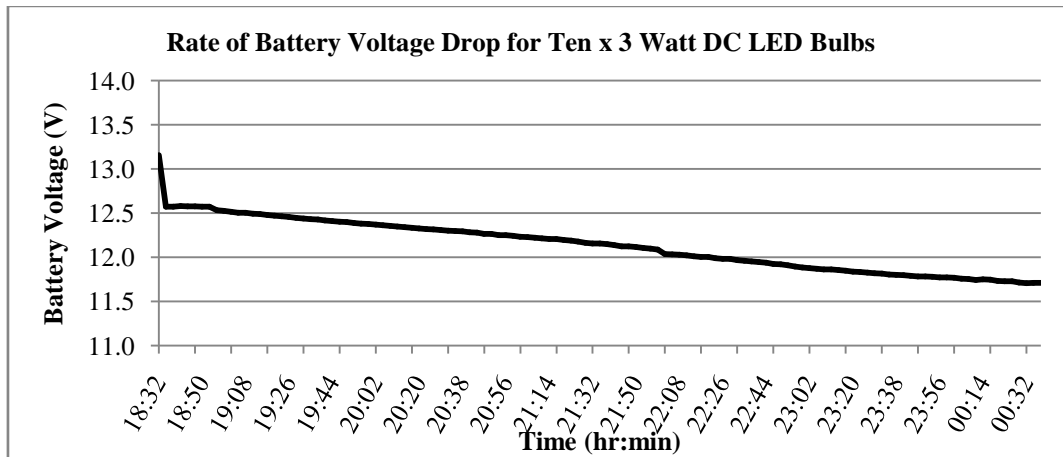


Fig.9. Rate of battery voltage drop for ten 3 W LED bulbs

IV. Conclusion

An efficient practicable and inexpensive charge controller was designed, constructed and implemented from relatively cheap PWM chips. It can be a replacement for more expensive PWM/MPPT brands available in the market. Test results obtained from each circuit demonstrate appreciable efficiencies as expected. The progressive cc-cv charging process was monitored at the non-inverting inputs of the error amplifiers of the TL494 chip. The charging circuit was found to charge faster with increasing insolation as higher currents are delivered by the MOSFET into the battery. Ten 3 Watt DC LED bulbs were powered for at least six hours each maintaining the same brightness. Increasing battery capacity to 24 Ah or more will be advantageous if more or higher wattage (5-7 Watt) LED bulbs are preferred. The PWM method used to drive the bulbs has proved more efficient than merely driving the LEDs directly from the battery. The product will be useful in rural districts or homes without grid such as a remote farmhouse.

References

- [1] TL494 Switch mode pulse width modulation control circuit. ON Semiconductor. [Online] Available at <http://onsemi.com> [Accessed November 16, 2007].
- [2] P. Griffith, Designing Switching Voltage Regulators with the TL494 Application Report SLVA001D. Texas Instruments. Rev. [Online] Available at: www.ti.com/lit/an/slva001e/slva001e.pdf [Accessed November 16, 2007].
- [3] J.H. Alberkrack, A simplified power supply design using the TL494 control circuit, AN983/D. [Online] Available at <http://onsemi.com> [Accessed October 22 2007].
- [4] I. Ozkaynak, Theory of operation of Ni-MH Battery Charger. [Online] Available at: <http://powerelectronics.com/site-files/powerelectronics.com/files/archive/powerelectronics.com/mag/606PET25.pdf> [Accessed April 4, 2015].
- [5] D. Schelle, and J. Castorena, Buck-Converter Design Demystified Power Electronics Technology. [Online] Available at: <http://powerelectronics.com/site-files/powerelectronics.com/files/archive/powerelectronics.com/mag/606PET25.pdf> [Accessed April 4, 2015].
- [6] B. Hauke, (2012) Basic Calculation of a Buck Converter's Power Stage. Texas Instruments Application Report SLVA77A. [Online] Available at: <http://www.ti.com/lit/an/slva477a/slva477a.pdf> [Accessed April 8, 2015].
- [7] Ejury, J. (2013) Buck Converter Design. Infineon Technologies North America (IFNA) Corp. [Online] Available at: <http://www.mouser.com/pdfdocs/buckconverterdesignnote.pdf> [Accessed April 8, 2015]
- [8] ROHM Semiconductor (2012) Inductor Calculation for Buck Converter IC, No.12027ECY01.[Online] Available at: http://rohms.rohm.com/en/products/databook/applinote/ic/power/switching_regulator/inductor_calculation_appli-e.pdf [Accessed April 8, 2015]
- [9] Texas Instruments Free Tool: Component Calculator for Buck Converters. [Online] Available at: <http://www.ti.com/tool/buck-convcalc>. [Accessed April 6, 2015]
- [10] Daycounter Inc. (2004) Buck Switching Converter Design Equations. [Online] Available at: <http://www.daycounter.com/LabBook/BuckConverter/Buck-Converter-Equations.phtml> [Accessed April 6, 2015].
- [11] TL431 Programmable Precision References. [Online] Available at <http://onsemi.com> [Accessed November 25, 2007].
- [12] T. van Roon 555 Timer Tutorial. Available at: <http://www.sentex.ca/~mec1995/gadgets/555/555.html>. [Accessed June 10 2012]
- [13] 12V Speed Controller/Dimmer. Available at:<http://www.diyelectronicsprojects.com/2013/01/circuit-diagram-12V-speed-controllerdimmer.html>. [Accessed August 7, 2014].
- [14] M. Kumar and D. Lama Design and development of cost effective automatic cut-off PV Charge Controller with indicator, IOSR-JEEE, 10(3) Ver iv, 2015,18-22
- [15] D. Abdulsalam, I. Mbamali, M. Mamman and Y.M. Saleh, An Assessment of Solar Radiation Patterns for Sustainable Implementation of Solar Home Systems in Nigeria. American International Journal of Contemporary Research, 2(6), 2012, 238-243.
- [16] C.O. Nwokocha, T.C. Chineke, and A.B. Fabenro, (2012) Renewable energy potentials for Nigeria: Making the transition from oil and gas to solar. Prime Journal of Physical Science. 1(4), 2012, 31-39.
- [17] Q. Wells, Smart Grid Home Cengage learning series in renewable energies, international edition, 2013, 171-177.
- [18] A.A.Willoughby, T.V. Omotosho, and A.P. Aizebeokhai, A simple resistive load I-V curve tracer for monitoring photovoltaic module characteristics. The Fifth International Renewable Energy Congress, (IREC), Hammamet, Tunisia, 2014, 14-PVE-75-P978-1-4799-2195-9/14/\$31.00©2014IEEE.